All-optical excitonic transistor

Y. Y. Kuznetsova,[1,*] M. Remeika,[1] A. A. High,[1] A. T. Hammack,[1] L. V. Butov,[1] M. Hanson,[2] and A. C. Gossard[2]

[1]Department of Physics, University of California at San Diego, La Jolla, California 92093-0319, USA
[2]Materials Department, University of California at Santa Barbara, Santa Barbara, California 93106-5050, USA
*Corresponding author: yuliyakuzn@gmail.com

Received December 21, 2009; revised March 19, 2010; accepted March 26, 2010;
posted April 6, 2010 (Doc. ID 121718); published May 5, 2010

We demonstrate experimental proof of principle for all-optical excitonic transistors where light controls light by using excitons as an intermediate medium. The principle of operation of all-optical excitonic transistors is based on the control of exciton fluxes by light. © 2010 Optical Society of America

OCIS codes: 200.3050, 230.1150, 230.3120, 250.3140.

Switches form the building blocks for circuit devices, and the development of optical and optoelectornic switches has been a subject of intensive research, see [1,2] for reviews. Recently, fast photonic switches have been realized [3–11]. Excitonic switches, i.e., switches using excitons—bound electron–hole pairs—as the operation medium, may offer a promising energy-efficient alternative to electrons in wires for future circuitry [12]. Potential advantages of excitonic devices include a high operation and interconnection speed, small dimensions, and the opportunity to combine many elements into integrated circuits [12–15]. Recently, a proof-of-principle demonstration of an exciton optoelectronic devices was reported [13–15]. The principle of operation of exciton optoelectronic devices is based on the control of exciton fluxes by electrode voltages.

The excitonic devices in [13–15] used indirect excitons as the operation medium. An indirect exciton is composed of an electron and a hole confined in spatially separated layers (Fig. 1a). The lifetime of indirect excitons exceeds by orders of magnitude the lifetime of regular excitons and increases exponentially with the separation d between the layers and the height of the separating barrier. Within their lifetime, indirect excitons can travel over large distances [16–22], for which devices can be patterned. Furthermore, indirect excitons have a built-in dipole moment ed. Therefore, an electric field F_z perpendicular to the quantum well (QW) plane results in the exciton energy shift $\delta E = edF_z$ [23]. This gives an opportunity to control the energy of indirect excitons by an electrode voltage.

Here, we present an all-optical excitonic transistor. In this device, all applied voltages are kept constant, and the exciton flux from source to drain is controlled optically by varying the light intensity at a photoconnector (PC) between two electrodes, which form an optically controlled gate.

A schematic of the transistor is shown in Figs. 1b and 1c. This proof-of-principle all-optical excitonic transistor has a photonic input, output, and control gate and uses indirect excitons as the operation medium. Photons transform into excitons at the input and travel from the input (source) to the output (drain) because of the potential energy change $\delta E \sim ed(F_{zd}-F_{zs}) \propto (V_d - V_s)$ created by the source voltage V_s and drain voltage V_d (Figs. 1b–1d). The exciton flux from source to drain is controlled by a light beam at a PC, which creates (removes) a barrier for the excitons in the region of the gate electrode when the transistor is off (on). Such optical control is implemented via varying the conductance of the PC and, as a result, voltage V_g in region g where the gate electrode crosses the exciton flux.

In two demonstrated devices, the PC was implemented in the form of a metal–semiconductor–metal photodetector with thirteen 10-μm-long, 0.6-μm-wide electrodes separated by 0.3 μm (Fig. 1e). The PC connected a split gate $g1$–$g2$. The electrode on the side opposite the PC was implemented in the form of a folded 2.4-mm-long, 0.5-μm-wide ribbon for device a and a folded 150-μm-long, 1-μm-wide ribbon for device b (Fig. 1e). Electrodes s and d were implemented in the form of 10 μm wide strips. The width of electrode g was 1 μm. The spacings between electrode g and electrodes s and d were 1 μm (Fig. 1e). Indirect

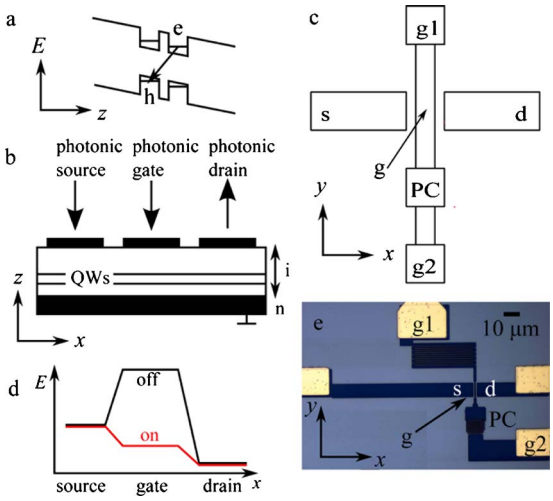

Fig. 1. (Color online) Principle of operation of the all-optical excitonic transistor. a, CQW diagram. b, c, Design schematic of the all-optical excitonic transistor. s, source; d, drain; $g1$–$g2$, split gate connected by a photoconnector (PC). The gate electrode crosses the exciton flux in region g. d, Schematic of the exciton potential energy. The exciton flux from source to drain is controlled by a light beam at the PC, which varies a barrier for the excitons in the region of the gate electrode. e, Top view of device b.

 © 2010 Optical Society of America

excitons were photocreated at the source s by a 690 nm diode laser within a 5 μm FWHM spot. The PC was controlled by either a 633 nm HeNe laser or a 786 nm diode laser focused to a 7 μm FWHM spot on the PC. $\lambda_{PC}=786$ nm corresponds to the energy of direct excitons in the structure. A direct exciton is composed of an electron and a hole in the same layer (Fig. 1a) and is characterized by a high oscillator strength. The experiments were done at 1.6 K. The structure was grown by molecular beam epitaxy. An n^+-GaAs layer with $n_{Si}=10^{18}$ cm^{-3} serves as a homogeneous bottom electrode. The top electrodes were fabricated by depositing a 100 nm semitransparent layer of indium tin oxide. A pair of 8 nm GaAs quantum wells separated by a 4 nm $Al_{0.33}Ga_{0.67}As$ barrier was positioned 0.1 μm above the n^+-GaAs layer within an undoped 1-μm-thick $Al_{0.33}Ga_{0.67}As$ layer. Positioning the coupled quantum wells (CQWs) closer to the homogeneous electrode suppresses the in-plane electric field [24], which otherwise can lead to exciton dissociation. The emission images were taken by a CCD with an interference filter covering the spectral range of the indirect excitons emitting in the vicinity of 800 nm. The spatial resolution was 1.5 μm.

Figure 2 presents images of the transistor emission and the corresponding emission intensity along the exciton flux in on and off states. When the light beam at the PC is off (Figs. 2a and 2c), the barrier at the gate electrode is essentially absent, and excitons can flow from source to drain: The transistor is on. The light beam at the PC creates a barrier for the exciton flux from source to drain at the gate (Figs. 2b and 2c); the transistor is off.

Figure 3 shows the emission intensity of indirect excitons integrated over output (drain) for various V_{g2} and, in turn, voltage difference $\Delta V=V_{g1}-V_{g2}$ at the split gate, for the gate control by a light on the PC with the wavelength $\lambda_{PC}=633$ (Fig. 3a) and 786 nm (Fig. 3b). For $\lambda_{PC}=633$ nm, the transistor works both for zero and nonzero ΔV. However, increasing the voltage on $g2$, and, in turn ΔV, results in a steeper change between ON and OFF and a higher ON–OFF ratio (Fig. 3a). The ON–OFF ratio of the signal integrated over the output (taken as the ratio of the signal when the laser at the PC is off to intensity when the laser at the PC is at 30 μW) is 8.5 for $V_{g2}=-5.0$ V, 9.5 for $V_{g2}=-2.5$ V, and 16.4 for $V_{g2}=0$ V for the device. The maximal electric currents through the device reach $\sim$10 μA under the illumination with $\lambda_{PC}=633$ nm so that the power dissipation reaches $\sim$100 μW.

For $\lambda_{PC}=786$ nm, the transistor works for nonzero ΔV (Fig. 3b). The ON–OFF ratio of the signal integrated over the output (taken as the ratio of the signal when the laser at the PC is off to intensity when the laser at the PC is at 180 μW) is 12 for $V_{g2}=0$ V for the device. The maximal electric currents through the device reach $\sim$1 μA under the illumination with $\lambda_{PC}=786$ nm; so the power dissipation reaches $\sim$10 μW.

The data are briefly discussed below. We first consider the variation of voltage V_g in region g due to the light-induced change of the PC resistance R_{PC}, which is defined as the resistance between g and $g2$ (Figs. 1c and 1e). In the absence of light on the PC, R_{PC} exceeds the resistance R of the electrode between $g1$ and g, $R_{PC}\gg R$ so that g is essentially disconnected from $g2$ and $V_g\approx V_{g1}$. A light on the PC photogenerates electrons and holes in the structure, which reduces R_{PC}, connecting $g1$ and $g2$ and shifting V_g toward V_{g2}, so that $V_g\approx V_{g2}$ for $R_{PC}\ll R$. To provide the on–off transistor operation, V_{g1} and V_{g2} were chosen such that making $V_g=V_{g2}$ ($V_g=V_{g1}$) creates (removes) a barrier for the excitons in region g; see Fig. 1d. This mechanism contributes to the transistor operation at nonzero ΔV.

Next we consider the variation of V_g due to the light-induced change of the resistance R_{PC-G} between the PC electrode on the top of the structure and the ground plane. In the absence of light on the PC, $R_{PC-G}\gg R$ and $V_g\approx V_{g1}$, while shining a light on the

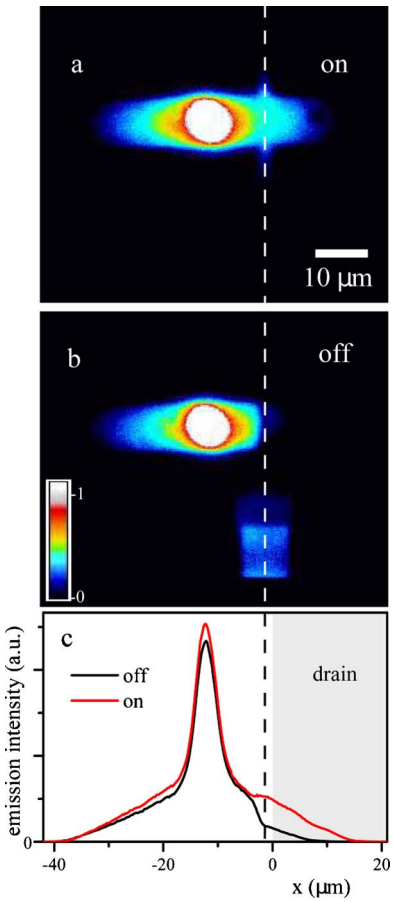

Fig. 2. (Color online) Operation of the all-optical excitonic transistor. Images of the exciton emission in, a, ON and, b, OFF states. $V_s=-4.5$, $V_d=-5.5$, and $V_{g1}=V_{g2}=-5.0$ V, device a. The circle shows the position of the laser excitation. The control light wavelength $\lambda_{PC}=633$ nm. Control light intensity is 0 in ON state in a and 30 μW in OFF state in b. A dashed line indicates the position of a gate electrode g. The control beam on the PC is revealed in b by the emission of indirect excitons created by it. c, Emission intensity of indirect excitons along the exciton flux for ON and OFF states corresponding to the false-color images in a and b. The gray area indicates the drain region. The contrast ratio of the output intensity integrated over the drain region is 8.5.

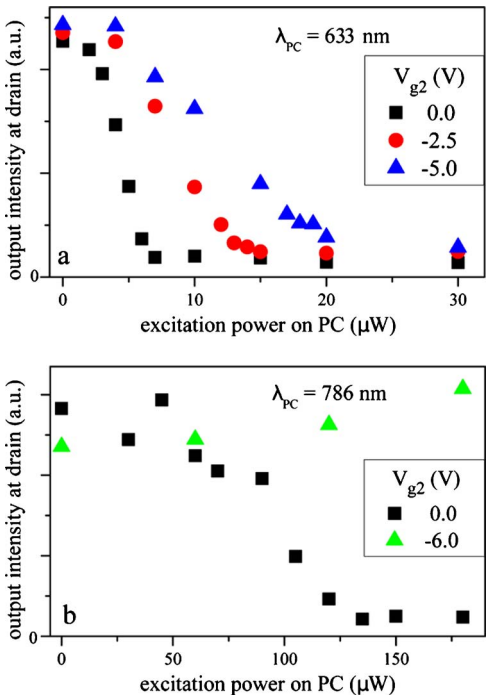

Fig. 3. (Color online) Output intensity integrated over the drain region versus intensity of control light on the PC for different V_{g2} for the control light wavelength, a, $\lambda_{PC}=633$ and b, 786 nm. In a, $V_s=-4.5$, $V_d=-5.5$, and $V_{g1}=-5.0$ V, device *a*. In b, $V_s=-5.5$, $V_d=-6.5$, and $V_{g1}=-6.0$ V, device *b*.

PC reduces R_{PC-G}, thus raising V_g by bringing it closer to the ground plate potential. This mechanism can become essential when the control light on the PC can substantially reduce R_{PC-G}, making it comparable and smaller than R and, as a result, leading to a change of V_g sufficient to vary the exciton flux. This mechanism contributes to the transistor operation both at zero and nonzero ΔV at $\lambda_{PC}=633$ nm. No switching due to such mechanism is observed when the PC is controlled by a 786 nm light ($\Delta V=0$, $V_{g2}=-6.0$ V in Fig. 3b). In this case, the photon energy is below the energy gap of the $Al_{0.33}Ga_{0.67}As$ layer in the structure, so electron–hole pairs are not photogenerated in this layer, and its resistance remains high ($R_{PC-G} \gg R$) when the PC is illuminated by the control light.

Excitons exist in the temperature range roughly below E_X/k_B (E_X is the exciton binding energy, k_B is the Boltzmann constant) [25], which limits the operation temperature. For the studied CQW structure, $E_X/k_B \sim 40$ K. For the AlAs/GaAs CQW in [15], $E_X/k_B \sim 100$ K and a proof of principle for the operation of optoelectronic excitonic transistors at $T \approx 100$ K was reported. E_X can be varied by choosing different semiconductor materials and structure parameters. Note also that high-quality samples with a low nonradiative recombination rate are required for optimal device operation. Characterization of device performance, as well as optimization of parameters, are subjects for future work.

In conclusion, we have demonstrated experimental proof of principle for all-optical excitonic transistors based on the modulation of exciton flux by light.

This work is supported by ARO and NSF. We thank Cal(it)^2 Nano3 staff for help with sample fabrication.

References

1. H. M. Gibbs, *Optical Bistability: Controlling Light with Light* (Academic, 1985).
2. K. Wakita, *Semiconductor Optical Modulators* (Kluwer Academic, 1998).
3. Y. Nishikawa, A. Tackeuchi, S. Nakamura, S. Muto, and N. Yokoyama, Appl. Phys. Lett. **66**, 839 (1995).
4. E. J. Gansen, K. Jarasiunas, and A. L. Smirl, Appl. Phys. Lett. **80**, 971 (2002).
5. A. Liu, R. Jones, L. Liao, D. Samara-Rubio, D. Rubin, O. Cohen, R. Nicolaescu, and M. Paniccia, Nature **427**, 615 (2004).
6. W. J. Johnston, M. Yildirim, J. P. Prineas, A. L. Smirl, H. M. Gibbs, and G. Khitrova, Appl. Phys. Lett. **87**, 101113 (2005).
7. Q. Xu, B. Schmidt, S. Pradhan, and M. Lipson, Nature **435**, 325 (2005).
8. Y. Jiang, W. Jiang, L. Gu, X. Chen, and R. T. Chen, Appl. Phys. Lett. **87**, 221105 (2005).
9. W. M. J. Green, M. J. Rooks, L. Sekaric, and Y. A. Vlasov, Opt. Express **15**, 17106 (2007).
10. J. Liu, M. Beals, A. Pomerene, S. Bernardis, R. Sun, J. Cheng, L. C. Kimerling, and J. Michel, Nat. Photonics **2**, 433 (2008).
11. H. W. Chen, Y. H. Kuo, and J. E. Bowers, Opt. Express **16**, 20571 (2008).
12. M. Baldo and V. Stojanovic, Nat. Photonics **3**, 558 (2009).
13. A. A. High, A. T. Hammack, L. V. Butov, M. Hanson, and A. C. Gossard, Opt. Lett. **32**, 2466 (2007).
14. A. A. High, E. E. Novitskaya, L. V. Butov, M. Hanson, and A. C. Gossard, Science **321**, 229 (2008).
15. G. Grosso, J. Graves, A. T. Hammack, A. A. High, L. V. Butov, M. Hanson, and A. C. Gossard, Nat. Photonics **3**, 577 (2009).
16. M. Hagn, A. Zrenner, G. Böhm, and G. Weimann, Appl. Phys. Lett. **67**, 232 (1995).
17. L. V. Butov and A. I. Filin, Phys. Rev. B **58**, 1980 (1998).
18. A. V. Larionov, V. B. Timofeev, J. Hvam, and K. Soerensen, Sov. Phys. JETP **90**, 1093 (2000).
19. L. V. Butov, A. C. Gossard, and D. S. Chemla, Nature **418**, 751 (2002).
20. Z. Vörös, R. Balili, D. W. Snoke, L. Pfeiffer, and K. West, Phys. Rev. Lett. **94**, 226401 (2005).
21. A. Gartner, A. W. Holleithner, J. P. Kotthaus, and D. Schul, Appl. Phys. Lett. **89**, 052108 (2006).
22. A. L. Ivanov, L. E. Smallwood, A. T. Hammack, S. Yang, L. V. Butov, and A. C. Gossard, Europhys. Lett. **73**, 920 (2006).
23. D. A. B. Miller, D. S. Chemla, T. C. Damen, A. C. Gossard, W. Wiegmann, T. H. Wood, and C. A. Burrus, Phys. Rev. B **32**, 1043 (1985).
24. A. T. Hammack, N. A. Gippius, S. Yang, G. O. Andreev, L. V. Butov, M. Hanson, and A. C. Gossard, J. Appl. Phys. **99**, 066104 (2006).
25. D. S. Chemla, D. A. B. Miller, P. W. Smith, A. C. Gossard, and W. Wiegmann, IEEE J. Quantum Electron. **20**, 265 (1984).

128.135.132.13 {ts '2017-07-27 19:23:45'}